Time-Resolved EPR Study of a 1,9-Flexible Biradical Dissolved in Liquid Carbon Dioxide. Observation of a New Spin-Relaxation Phenomenon: Alternating Intensities in Spin-Correlated Radical Pair Spectra

Nikolai I. Avdievich, Katerina E. Dukes, Malcolm D. E. Forbes,* and Joseph M. DeSimone

Venable and Kenan Laboratories, Department of Chemistry, CB No. 3290 University of North Carolina, Chapel Hill, North Carolina 27599

Received: July 2, 1996; In Final Form: October 9, 1996[⊗]

X-band (9.5 GHz) time-resolved electron paramagnetic resonance (TREPR) spectra of a 1,9-acyl−alkyl biradical were obtained at room temperature in benzene and in liquid (950 psi) carbon dioxide (CO_2) solutions. The spin exchange interaction (J) in this biradical is negative and larger in magnitude than the hyperfine interaction (q). This leads to the observation, in both solvents, of spin-correlated radical pair (SCRP) spectra which are net emissive. Spectra obtained at later delay times (>1.5 μs) in CO_2 exhibit alternating intensities of their SCRP transitions due to spin relaxation but do not show any significant change in line width. The same effect is observed in benzene, but on a slower time scale. Q-band (35 GHz) experiments in benzene showed that the phenomenon was found to be both field and temperature dependent. It is also chain-length dependent, being much stronger in short biradicals ($<C_{10}$). A Redfield theory analysis of the spin-state populations is presented and discussed that includes J modulation, electron dipole−dipole interaction modulation, and uncorrelated relaxation mechanisms (hyperfine and g-factor anisotropies). Using this model, simulation of the Q-band time dependence at 64 °C, along with a careful consideration of several relaxation parameters, leads to the conclusion that hyperfine-dependent J modulation relaxation, coupled with the dipolar mechanism and $S-T^-$ mixing, is responsible for the observed effects.

Introduction

In a series of recent papers,[1] we have demonstrated that in time-resolved (CW) electron paramagnetic resonance (TREPR) spectroscopy of spin-correlated radical pairs and biradicals (SCRPs), dynamic or motional effects can exert a large influence on the spectral appearance. This applies to spin-relaxation phenomena such as J modulation, which leads to alternating line widths[1a,1b] and also to chemically induced electron-spin-polarization (CIDEP) mechanisms, where changes in viscosity can lead to differences in competition between the various mechanisms.[1d] For example, in long biradicals at low temperatures, we have observed that the radical pair mechanism (RPM) of CIDEP becomes stronger than the SCRP mechanism due to the increased viscosity in low-temperature organic solvents.[1c]

All of our previous studies of dynamic effects were carried out in "conventional" solvents over a wide temperature range. However, the viscosities of these solutions were never less than 0.5 cP. Liquid carbon dioxide, CO_2, is an unusual solvent in that it has a very low viscosity (approximately 0.06 cP at ambient temperatures and 800−2000 psi pressure), placing it somewhere in between a conventional solvent and a gas. Furthermore, liquid and supercritical fluid CO_2 have gained attention for their roles in separation science[2] and in free-radical polymerization chemistry.[3] For these reasons, we have embarked upon a research program aimed at understanding the magnetic and kinetic properties of free radicals and biradicals in liquid and supercritical CO_2 and to use the unique properties of this solvent, such as its pressure-tunable viscosity and density, to examine well-established spin-polarization mechanisms at the other end of the viscosity spectrum from "normal" solvents.

In this paper, we present the results of a TREPR study of spin relaxation in a 1,9-bis(alkyl) biradical, whose structure and photochemical production using laser flash photolysis are shown in Scheme 1. In separate publications, we will describe (1) the detail construction of our apparatus for performing TREPR at high pressures and variable temperatures,[4] (2) the large solvent effect of CO_2 on the spin exchange interaction in acyl−alkyl biradicals,[5] and (3) preliminary studies of polymer free-radical initiator kinetics and RPM spin-polarization production in CO_2 vs conventional solvents such as benzene and several fluorocarbons and chlorofluorocarbons (CFCs).[6]

SCHEME 1

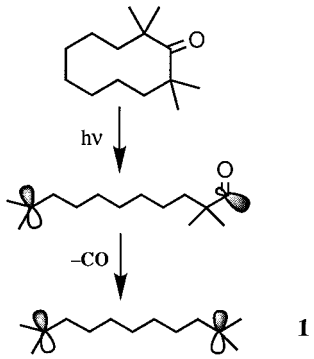

1

Experimental Section

Our setups for TREPR at X-band[7] (9.5 GHz) and Q-band[8] (35 GHz) have been described previously. The UV-transparent, high-pressure flow cell is a 9-mm-o.d., 2-mm-i.d. optical-grade quartz tube that has been epoxied at each end to stainless steel pressurizing heads. These heads are in turn connected via $^1/_{16}$-in. stainless steel tubing to a high-pressure pump and a reservoir equipped with sapphire windows to allow visualization of the sample during flow. A high-pressure syringe capable of withstanding pressures of 30 000 psi is used to pressurize the

* To whom correspondence should be addressed.

[⊗] Abstract published in *Advance ACS Abstracts,* December 15, 1996.

S1089-5639(96)01947-0 CCC: $14.00

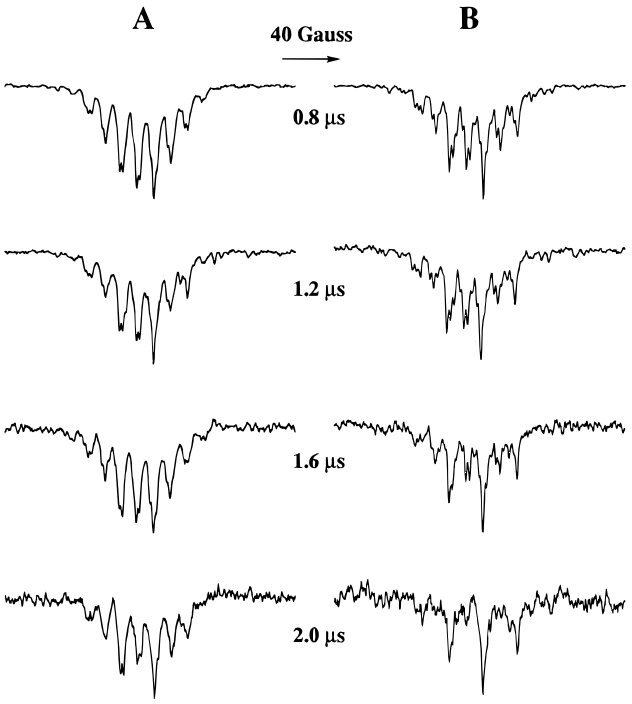

Figure 1. Experimental X-band TREPR spectra of biradical **1** in (A) benzene and (B) liquid CO_2 at 950 psi. The experimental spectra were obtained upon photolysis of a 50 mM solution of precursor ketone at a temperature of 28 °C and the delay times indicated.

flow system after introduction of the desired solute into the reservoir. About 1 h of equilibration time is necessary before EPR data can be collected. This ensures a stable pressure, temperature, and a flat EPR baseline. The X-band microwave resonator is a home-built brass TE_{011} cylindrical cavity with tunable aluminum endplates which are positioned to bring the resonator, with sample and flow tube, into the range of the microwave source. A grid to provide light access was constructed by machining horizontal slices through the cavity. A Kevlar safety shield, 1-in. thickness, was used when pressure testing the cell to at least 3000 psi for 1 h, after which the cell was placed in the cavity, which is 0.5-in.-thick brass and acts as its own shield. A thick-walled cavity can be used for these studies because field modulation is bypassed in TREPR spectroscopy. The operating pressure during all experiments was at least 50% lower than the highest test pressure.

Prior to each high-pressure experiment, the entire flow system was flushed with a variety of organic solvents and purged with dry nitrogen gas. The precursor ketone (2,2,10,10-tetramethylcyclodecanone) was synthesized from cyclodecanone (Lancaster) using standard alkylation chemistry. It is a white crystalline solid at ambient temperature and pressure. UV-grade benzene was used without further purification, and dry CO_2 (SCF/SFE Grade) was purchased from Air Products and Chemicals, Inc.

Results

Figure 1 shows X-band TREPR data of biradical **1** as a function of delay time after the excimer laser flash (308 nm, 17 ns, 10 mJ). The data in Figure 1A were obtained in benzene solution, while those in Figure 1B were obtained in liquid CO_2 at a temperature of 28 °C and a pressure of 950 psi. At early delay times in both solvents, the signals appear typical of short bis(alkyl) biradicals with SCRP polarization: net emissive from $S-T^-$ mixing and half the hyperfine coupling due to the large J coupling. However, the time evolution of these signals in

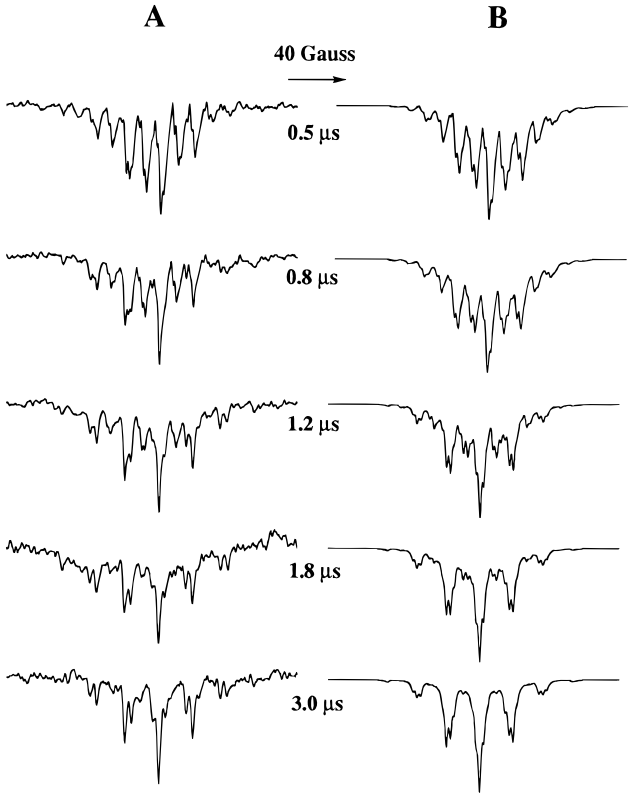

Figure 2. (A) Experimental and (B) simulated Q-band TREPR spectra of biradical **1**. The spectra in A were obtained upon photolysis of a 50 mM solution of precuror ketone in benzene at a temperature of 64 °C. The parameters used in the simulations are listed in Table 1.

the two solvents proceeds very differently. In CO_2, the biradicals lose intensity from every other packet of lines in the spectrum, leading to a pattern of alternating intensities from low to high field. Note that the line widths appear to remain fairly constant over this time range. Considering the low viscosity of CO_2, it seems likely that chain dynamics will be different in this unusual solvent and that this could lead to unusual spin polarization or relaxation. Furthermore, the phenomenon observed here seems to affect only the intensities and not the line widths. This has led us to focus our attention on T_1 spin-relaxation mechanisms (population transfer) as the cause of this interesting effect.

If population transfer between the triplet levels is important, then running the experiment at a different magnetic field should alter the relaxation rate.[9] Figure 2A shows the time dependence obtained for biradical **1** in benzene at Q-band. Unfortunately, we are not presently equipped to perform high pressure experiments at Q-band. However, the results in Figure 2A clearly show that the alternating intensities effect is indeed stronger at this field. These data were also taken at a higher temperature than that in Figure 1A, but a comparison of data obtained at the same temperature shows that there are still large differences in the effect at the two spectrometer frequencies. Data from the higher temperature experiment are displayed here because they showed the best signal to noise ratio and are the dataset most representative of the effect. A simulation of the Q-band time dependence is shown in Figure 2B, and the theoretical model leading to this result will be discussed in the next section.

Discussion

In a previous publication, we considered the effects of J modulation by conformational motion on T_1 in flexible biradicals

SCHEME 2

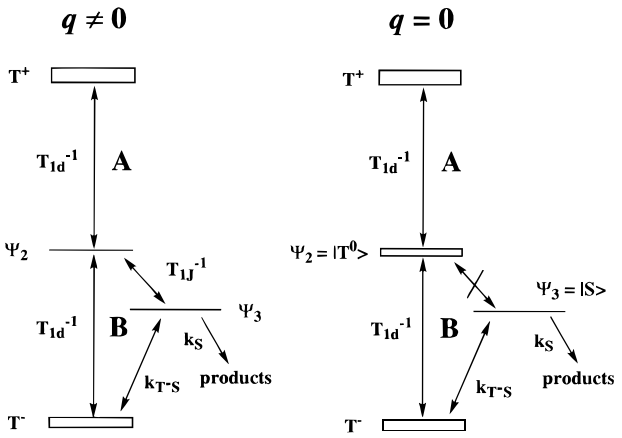

in organic solvents.[1a,1b] In that work, we found that this T_1 mechanism was relatively unimportant, but it played a large role in determining T_2 for certain SCRP transitions. Its contribution to T_1 will be reconsidered here in light of the different chain dynamics expected in CO_2. Two other spin-relaxation mechanisms are possible in biradicals: (1) modulation of the electron dipole−dipole interaction and (2) uncorrelated relaxation due to hyperfine and *g*-factor anisotropies. These two mechanisms have been considered in an earlier paper by de Kanter et al.[10] on the magnetic field dependence of chemically induced dynamic nuclear polarization (CIDNP) in acyl−alkyl biradicals performed using NMR spectroscopy. Here we have incorporated all three mechanisms into our SCRP simulation routine to attempt to reproduce the time-dependent behavior in Figure 1B and Figure 2A. The behavior is complex, and it is appropriate to begin our discussion of the results by presenting the relaxation model in more detail.

We begin with an overview of SCRP theory, as illustrated by the level diagram in Scheme 2. Conventional SCRP theory[11] uses kinetic differential equations for the diagonal elements of the density matrix ρ_{11}, ρ_{22}, ρ_{33}, and ρ_{44} with the states described by a basis set consisting of the wave functions (with their eigenvalues)

$$|1\rangle = |\mathrm{T}^{+}\rangle \qquad E_1 = -J + \Omega \tag{1a}$$

$$|2\rangle = \cos\theta|\mathrm{S}\rangle + \sin\theta|\mathrm{T}^{0}\rangle \qquad E_2 = \Omega \tag{1b}$$

$$|3\rangle = -(\sin\theta)|\mathrm{S}\rangle + \cos\theta|\mathrm{T}^{0}\rangle \qquad E_3 = -\Omega \tag{1c}$$

$$|4\rangle = |\mathrm{T}^{-}\rangle \qquad E_4 = -\mathrm{J} - \Omega \tag{1d}$$

where $\Omega = (q^2 + J^2)^{1/2}$, $\tan 2\theta = q/J$, and the other variables have their conventional meanings: $|\mathrm{S}\rangle$, $|\mathrm{T}^{+}\rangle$, $|\mathrm{T}^{0}\rangle$, and $|\mathrm{T}^{-}\rangle$ are the standard singlet and triplet spin basis functions, *J* is the spin-exchange interaction, and *q* is the local magnetic field difference between the radical centers, consisting of hyperfine interactions and *g*-factor differences. For the biradical studied here, $\Delta g = 0$; therefore, *q* is determined exclusively by the hyperfine coupling terms. The *q* term is very important in our analysis since it is clear that the relaxation mechanism we are observing affects some hyperfine lines differently than others; i.e., we need to consider *q*-dependent processes.

The "kinetic" approach to the density matrix method is reasonable since a large value of the reencounter rate constant, k_{en}, ($>10^9$ s^{-1}), leads to a fast dephasing rate, destroying the off-diagonal elements of the density matrix at the times much shorter than our experimental observation time.[12] k_{en} is very fast indeed for the short-chain-length C_9 bis(alkyl) biradical under discussion in this paper. The energies and populations of the four electronic sublevels are shown in Scheme 2 for two cases: (left) when $q \neq 0$ and (right) when $q = 0$.

To calculate the rate constants for *J* modulation, dipole−dipole, and uncorrelated relaxation mechanisms, we have applied Redfield theory[13] as in the work of de Kanter et al.[10] on simulations of magnetic field effects in CIDNP data on similar biradicals and as was used in our previous work.[1a] Since this approach is based on perturbation theory, it must be used carefully. The criterion for the validity of Redfield theory is written as

$$\langle V^2\rangle^{1/2}\tau_c < 1 \tag{2}$$

Here *V* is a general time-dependent matrix element inducing the transitions and τ_c is its correlation time. We now make a few estimations about the magntiude of these parameters in our biradical for *J* modulation relaxation. We define the matrix element for *J* modulation as V_J. As in our previous paper, the use of end-to-end distance distributions, along with an exponentially decaying function for *J* with distance, $J = J_0 \exp(-\lambda(r - r_0))$, allows us to estimate this parameter for a given chain length. Using $\lambda = 1.1$ Å^{-1} and $r_0 = 3.5$ Å, we have determined that $\langle V_J^2\rangle^{1/2} \sim J$ for most short biradicals (C_7−C_9). The value we have used for V_J and *J* in our calculated spectra is 1500 G. Next we estimate that the correlation time for *J* modulation, τ_e, is about 2×10^{-11} s, a reasonable value for alkane chain jump times at these temperatures and in these solvents. Using these values, we obtain the result that $\langle V_J^2\rangle^{1/2}\tau_e$ is about 0.3. While this is close to the limit of the validity of the theory, we can still use it to explain the observed phenomena.

J modulation relaxation not only affects broadening of selected SCRP transitions in biradical TREPR spectra but also causes population relaxation between sublevels |2> and |3> according to eqs 3a and 3b.

$$R^{J}_{22,33} = \frac{2\langle V_J^{\,2}\rangle q^2}{\Omega^2} k(2\Omega) \tag{3a}$$

$$k(\omega) = \frac{\tau_e}{1 + \omega^2 \tau_e^{\,2}} \tag{3b}$$

The Redfield relaxation element for this process is given in eqs 3a and 3b. Since the relaxation rate T_1^{-1} is proportional to the *q* value, there are no transitions between states |2> and |3> due to this relaxation mechanism for biradicals with the same nuclear spin numbers at both radical centers, i.e., when $q = 0$.

We now consider population relaxation caused by modulation of the electron dipole−dipole interaction. This mechanism can effect the transitions $|\mathrm{T}^{+}\rangle \leftrightarrow |2\rangle$ and $|\mathrm{T}^{-}\rangle \leftrightarrow |2\rangle$, i.e., transitions between states with substantial triplet character. The matrix element for this process, which is the same for each of the two transitions, is shown in

$$R^{\mathrm{d}}_{22,++} = \frac{3\langle V_{\mathrm{d}}^{\,2}\rangle \sin^2\theta}{10} k(\omega_{2+}) \tag{4a}$$

$$V_{\mathrm{d}}^{\,2} = \frac{g^4\beta^4}{h^2 r^6} \tag{4b}$$

The dipole−dipole interaction also connects states |2> and |3>. The relaxation matrix element is given by

$$R^{\mathrm{d}}_{22,33} = \frac{\langle V_{\mathrm{d}}^{\,2}\rangle q^2}{10\Omega^2} k(\omega_{23}) \tag{5}$$

The ratio q^2/Ω^2 that appears in eq 5 causes this matrix element

TABLE 1: Kinetic and Magnetic Parameters Used for Simulations in Figure 2B

		J modulation		dipole−dipole		uncorrelated		
J, MHz	k_{en}	$\langle V(t)^2\rangle^{1/2}$, MHz	τ_e, s	$\langle V(t)^2\rangle^{1/2}$, MHz	τ_d, s	$\langle V(t)^2\rangle^{1/2}$, MHz	τ_u, s	natural line width,[a] G
-4200	5×10^9	8400	10^{-11}	280	10^{-11}	56	10^{-11}	2.5−3.0

[a] Line widths are a function of delay time and were varied over this range.

to be quite small. This is because the *J* value obtained from our simulations is about 1500 G (vide infra), and *q* is about 20 G, with the result that this factor decreases the matrix element by about 2 orders of magnitude. Although eq 3a also contains this ratio for T_1 relaxation between states |2> and |3> via *J* modulation, the matrix element for *J* modulation, V_J, is substantially larger in this biradical than the matrix element for dipole−dipole relaxation, V_d, between these two states. This allows us to exclude $R^d_{22,33}$ from further consideration. We conclude from this analysis that the most important *q*-dependent T_1 relaxation channel connecting sublevels |2> and |3> is *J* modulation. For reasonable values of *q* for organic radicals (about 30 G or 100 MHz), a correlation time τ_e of about 10^{-11} s, and by assuming (as discussed above) that $\langle V^2\rangle^{1/2} \sim J$, we estimate that T_{1J}^{-1} is approximately 10^7 s^{-1}. This is at least an order of magnitude faster than any other relaxation rate for transitions between states |2> and |3>. Because of the *q* dependence of T_{1J}^{-1}, there is therefore a large difference in relaxation rate for subensembles with $q = 0$ and $q \neq 0$. The overall appearance after a few microseconds is an alternation of line intensities in the TREPR spectra. Note that this is a very different polarization pattern from the alternating line width patterns which are created by *J* modulation via a T_2 process.

The uncorrelated relaxation matrix element $R^u_{22,33}$ has been described previously by de Kanter et al.[9] and is shown in eq 6.

$$R^u_{22,33} = \langle V_u^2\rangle k(\omega_{23}) \tag{6}$$

It is important to note that the uncorrelated matrix element does not show any dependence on *q*. The matrix element V_u arises from hyperfine or *g*-factor anisotropy. An interesting feature of the present system is that all three relaxation mechanisms have nonzero $R_{22,33}$ matrix elements, which connect ρ_{22} and ρ_{33}.

For large *J* values (i.e., $J \gg q$) the resonant frequencies for transitions A and B in Scheme 2 are the same within the limit of line widths. The total line intensity is proportional to the sum of two population differences: that between |T−> and state |2>, $(n_{T-} - n_2)$, and that between state |2> and |T+>, $(n_2 - n_{T+})$. This sum works out to be $n_{T-} - n_{T+}$, or the difference in population between |T+> and |T−>. In the completely symmetric case, when all the rates for transitions from |T−> or |T+> to |T0> or |S> are the same, the line intensities are determined only by the population difference between |T+> and |T−>. So, the population of the |T0> state becomes unimportant. However, S−T− mixing, which can be dominant in the large *J* case, can lead to a dependence of line intensities on the transition rates between states |2> and |3>. Or, in other words, S−T− transitions break the symmetry of the |T+> and |T−> states. Also important is that, in the presence of sufficiently fast population relaxation (T_{1J}^{-1} in Scheme 2), *J* modulation can significantly decrease the lifetime of biradicals with $q \neq 0$. The above-mentioned conditions can lead to the observed effect of different decay rate constants for biradicals with $q = 0$ and $q \neq 0$. To obtain more quantitative information about relaxation rates and correlation times, a more detailed kinetic analysis is required, which is currently underway in our laboratory.

Now we are equipped, using eqs 3, 4, and 6, to calculate rates for the |T+> ↔ |2>, |T+> ↔ |3>, |2> ↔ |T−>, and |3> ↔ |T−> transitions for all three T_1 relaxation mechanisms. Figure 2B shows a simulation of the time dependence of the Q-band TREPR spectra of **1** shown in Figure 2A. The parameters used in the simulation are listed in Table 1. The combination of T_1 relaxation by *J* modulation, which causes transitions between sublevels |2> and |3>, and dipolar T_1 relaxation transitions |T+> ↔ |2> and |2> ↔ |T−> reproduces the effect of alternating line intensities in the biradical spectra very well.

Interestingly, both uncorrelated and dipole−dipole relaxation mechanisms lead to the same effect. Increasing the rate of any of the three relaxation pathways causes an increase of the relative decay rate of the transitions corresponding to biradicals with $q \neq 0$. However, uncorrelated relaxation leads to alternating intensities only when the two matrix elements $R^u_{11,33}$ and $R^u_{33,44}$, corresponding to transitions between energy levels |T+> ↔ |3> and |3> ↔ |T−>, respectively, have approximately the same value. This situation can only occur when the relaxation rate constants do not depend on the Larmor frequency values, i.e., $\omega_0\tau_u < 1$. At Q-band (35 GHz), this means the correlation time for uncorrelated relaxation, τ_u, should be smaller than 5×10^{-12} s. At X band (9.5 GHz), it should be smaller than 2×10^{-11} s. If the motion leading to uncorrelated relaxation is the movement of the end of the chain (e.g., methyl group rotation), these are reasonable upper limits for τ_u.

In contrast, electron dipole−dipole relaxation leads to this effect at any value of the correlation time, τ_d, because this mechanism does not effect transitions between sublevels |T+> or |T−> and sublevel |3>. In a short alkyl chain, there may also be a very short correlation time for the dipolar mechanism. For this reason, it might be considered difficult to separate the dipolar and uncorrelated relaxation channels. However, because the phenomenon of alternating intensities is observed only for short-chain-lenth biradicals (less than 10 carbon atoms), we conclude that dipole−dipole relaxation is more likely to be the active mechanism. Chain-length dependent uncorrelated relaxation would be extremely unusual, and we do not see the alternating intensities in C_{16} biradicals in either solvent. We therefore do not consider the uncorrelated mechanism further.

The electron dipole−dipole interaction can be modulated either by tumbling of the entire biradical with a slow correlation time ($\tau_d > 10^{-10}$ s) or by fast rotation around each single bond ($\tau_d \sim (1-5) \times 10^{-11}$ s). For a slow correlation time with an upper limit of about 1×10^{-10} s at the X-band microwave frequency, the factor $\tau_d/(1 + \omega_0^2\tau_d^2)$ is about 2.5×10^{-12} s, which would lead to T_1^{-1} values that are too slow to account for the observed effects. We can therefore neglect the contribution of the rotation of the whole biradical and consider only the short correlation time for dipole−dipole relaxation. As shown in Figure 2, increasing the temperature to 64 °C at Q-band leads to a more pronounced alternating intensity effect. This allows us to conclude that the correlation time τ_d has to be longer than ω_0^{-1}, or 5×10^{-12} s, which is reasonable. Differences in decay rate constants observed in X-band experiments between benzene and liquid CO_2 lead to the same conclusion, and ω_0^{-1} leads to an even higher estimated lower limit for τ_d of about 2×10^{-11} s.

It is also difficult to separate dipole−dipole and *J* modulation relaxation contributions. They are necessarily coupled due to the fact that they are both functions of the end-to-end distance

fluctuations of the alkyl chain. One possible way to separate their contributions to the alternating intensity effect is to run the experiments at different temperatures and magnetic fields. Since the energy gaps for both relaxation rate constants are so different, they could give different contributions at different temperatures, i.e., to investigate T_1 as a function of different correlation times. Experiments at different magnetic fields also might be very helpful. Since the energy gap between sublevels $|2>$ and $|3>$ is determined only by the *J* value, the *J* modulation relaxation rate constant will remain the same at X- and Q-band frequencies. But dipole−dipole relaxation leading to transitions $|T^+> \leftrightarrow |2>$ and$|\ 2> \leftrightarrow |T^->$ may change significantly at higher fields, if the correlation time τ_d is larger than ω_0^{-1}. It will also be useful to study this phenomenon in biradicals with different chain lengths. Since dipole−dipole and exchange interactions have different distance dependencies, the matrix elements will increase with the shortening of chain length. These experiments are presently underway in our laboratory. Further investigations of SCRP polarization and relaxation mechanisms in CO_2 are also being pursued.

Acknowledgment. This work was supported by the National Science Foundation Chemistry Division (Grant No. CHE-9522007), the NSF National Young Investigator Program (M.D.E.F., 1993−1998, Grant No. CHE 9357108), and the NSF Presidential Faculty Fellows Program (J.M.D., 1993−1997).

References and Notes

(1) (a) Avdievich, N. I.; Forbes, M. D. E. *J. Phys. Chem.* **1995**, *99*, 9660. (b) Avdievich, N. I.; Forbes, M. D. E. *J. Phys. Chem.* **1996**, *100*, 1993. (c) Forbes, M. D. E.; Avdievich, N. I.; Ball, J. D.; Schulz, G. R. *J. Phys. Chem.* **1996**, *100*, 13887. (d) Tominaga, K.; Yamauchi, S.; Hirota, N. *J. Phys. Chem.* **1988**, *88*, 553.

(2) McHugh, M. A.; Krukonis, V. J. *Supercritical Fluid Extraction*; Butterworth-Heinemann: Boston, 1994.

(3) (a) DeSimone, J. M.; Maury, E. E.; Menceloglu, Y. Z.; McClain, J. B.; Romack, T. J.; Combes, J. R. *Science* **1994**, *265*, 356. (b) Clark, M. R.; DeSimone, J. M. *Macromolecules* **1995**, *28*, 3002. (c) Kapellen, K. K.; Mistele, C. D.; DeSimone, J. M. *Macromolecules* **1996**, *29*, 495.

(4) Dukes, K. E.; Forbes, M. D. E.; DeSimone, J. M. To be published.

(5) Forbes, M. D. E.; Dukes, K. E.; Avdievich, N. I.; DeSimone, J. M. Submitted for publication.

(6) Dukes, K. E.; Forbes, M. D. E.; DeSimone, J. M. To be published.

(7) (a) Forbes, M. D. E. *J. Phys. Chem.* **1993**, *97*, 3390. (b) Forbes, M. D. E. *J. Phys. Chem.* **1993**, *97*, 3396.

(8) Forbes, M. D. E. *Rev. Sci. Instrum.* **1993**, *64*, 397.

(9) Abragam, A. *The Principles of Nuclear Magnetism*; Clarendon Press: Oxford, 1961; p 264 ff.

(10) de Kanter, F. J. J.; den Hollander, J. A.; Huizer, A. H.; Kaptein, R. *Mol. Phys.* **1977**, *34*, 857.

(11) (a) Closs, G. L.; Forbes, M. D. E.; Norris, J. R., Jr. *J. Phys. Chem.* **1987**, *91*, 3592. (b) Buckley, C. D.; Hunter, D. A.; Hore, P. J.; McLauchlan, K. A. *Chem. Phys. Lett.* **1987**, *135*, 307.

(12) (a) Koptyug, I. V.; Lukzen, N. N.; Bagryanskaya, E. G.; Doctorov, A. B. *Chem. Phys. Lett.* **1990**, *175*, 467. (b) Shushin, A. I. *Chem. Phys. Lett.* **1991**, *181*, 274.

(13) Redfield, A. G. *IBM J. Res. Dev.* **1957**, *1*, 19.